



Aspergillus nidulans RhoA is involved in polar growth, branching, and cell wall synthesis

Gretel M. Guest, Xiaorong Lin, and Michelle Momany*

Department of Plant Biology, University of Georgia, Athens, GA 30602, USA

Received 24 April 2003; accepted 26 August 2003

Abstract

Growth of the filamentous fungus *Aspergillus nidulans* begins when the conidium breaks dormancy and grows isotropically. Eventually a germ tube emerges and the axis of growth remains fixed in the primary hypha while new growth axes are established basally to form secondary germ tubes and lateral branches. Rho1 is a Rho family GTPase that has been shown to be involved in polarity establishment and cell wall deposition in *Saccharomyces cerevisiae*. A gene predicted to encode a Rho1 homolog was cloned from *A. nidulans* and named *rhoA*. Strains carrying ectopic copies of the constitutively active *rhoA*^{G14V} allele or the dominant *rhoA*^{E40I} allele were created and characterized. The constitutively active *rhoA*^{G14V} strain grew slowly relative to wild type and showed an abnormal clustered pattern of branch emergence. The *rhoA*^{G14V} strain also labeled intensely with calcofluor, showed elevated levels of cell wall *N*-acetylglucosamine and had unusually thick cell walls. The dominant *rhoA*^{E40I} strain was accelerated in the emergence of secondary and tertiary germ tubes, and lateral branches relative to wild type and showed lysis with prolonged incubation. The *rhoA*^{E40I} strain also was hypersensitive to the cell wall disrupting agents calcofluor and caspofungin acetate and showed an increase in cell wall *N*-acetylglucosamine levels. Our results suggest that *rhoA* plays a role in polarity, proper branching pattern, and cell wall deposition.

© 2003 Elsevier Inc. All rights reserved.

Keywords: Polar growth; RhoGTPase; Rho1; Cell wall

1. Introduction

In multicellular fungi polar extension is needed for vegetative growth and the development of complex tissues and sexual structures. *Aspergillus nidulans* is a good model organism for the study of polar growth in filamentous fungi because of its well developed genetic system and defined early growth pattern. In *A. nidulans*, morphogenetic landmarks have been correlated with the duplication cycle and a stepwise growth pattern has been characterized (Harris, 1997; Momany and Taylor, 2000). A conidium breaks dormancy when it contacts appropriate signals from the environment (Osherov and May, 2001). The conidium initially expands isotropically, but soon switches to polar growth. The primary germ tube emerges and growth is directed apically. A

secondary germ tube emerges, usually in a bipolar pattern, and a septum is laid down at the base of the primary germ tube. As growth continues, the hyphae become compartmentalized with the addition of more septa and lateral branches emerge from basal compartments.

Much is known about polar growth in the budding yeast *Saccharomyces cerevisiae* and its tight coordination with the cell cycle (reviewed by Lew and Reed, 1995). A yeast cell grows isotropically in G1. The products of *BUD* and *CDC42* genes establish the axis of growth and the bud emerges at the G1/S boundary. An apical to isotropic switch in the daughter bud occurs in G2. Finally, growth is redirected to the mother-bud neck late in M phase and the two yeast cells separate.

Much less is known about polar growth in filamentous fungi (Momany, 2002). Attempts to obtain null mutants of homologs of the polarity establishment gene *CDC42* in the filamentous fungi *Ashbya gossypii* and *Penicillium marneffeii* were unsuccessful suggesting such

* Corresponding author. Fax: 1-706-542-1805.

E-mail address: momany@botany.uga.edu (M. Momany).

deletions are lethal (Boyce et al., 2001; Wendland and Philippsen, 2001). Conidia from *A. gossypii* heterokaryons containing deleted *Agcdc42* had depolarized actin and grew isotropically for a short time before they died. In contrast, overexpression of dominant mutant alleles of the *P. marneffei CDC42* homolog, *cflA*, caused varied phenotypes including decreased rates of germination and increased rates of germ tube emergence.

Polarity maintenance, the continued deposition of secretory vesicles, wall remodeling and growth at the tip, is a process that is also not well understood in filamentous fungi. Cytological studies in *A. nidulans* and *Neurospora crassa* clearly show the involvement of actin, tubulin and the Spitzenkörper in apical growth (Harris, 1997; Riquelme et al., 2002). Unlike yeast, growth continues at the apex in filamentous fungi even though a new axis of growth can be established through secondary germ tubes or branches.

Though little is known about the genes governing branching, it is likely that branch emergence uses polarity establishment and maintenance steps similar to those used in germ tube emergence (Momany, 2002). Two *A. nidulans* proteins that have been implicated in branching are AspB, a septin and SepA, a formin. Both localize to the site of pre-emergent secondary germ tubes and lateral branches in an actin dependent manner (Sharpless and Harris, 2002; Westfall and Momany, 2002).

Polar growth requires the deposition of new cell wall. The well-characterized *S. cerevisiae* cell wall is made up of polymerized chains of (1–3) β -D-glucans. Attached to the non-reducing ends of the (1–3) β -D-glucan polymers are (1–6) β -D-glucans, chitin and cell wall proteins (Lipke and Ovalle, 1998).

In *S. cerevisiae* and *Schizosaccharomyces pombe* the RhoGTPases have extensive involvement in polar growth and cell wall synthesis. The family of RhoGTPases (named “rho” for ras homology) are members of the larger ras superfamily, also known as small GTPases (Hall, 2000). The membrane-bound Rho subfamily is highly conserved in all eukaryotes so far examined, and is comprised of Rho, Rac, and Cdc42. RhoGTPases, like other GTPases, function as “on/off” molecular switches. When RhoGTPase is bound to GTP, the GTPase is activated and affects downstream effectors. When bound to a GDP molecule, the GTPase is deactivated. The intrinsic rate of GTP–GDP exchange in these proteins is low. Guanine nucleotide exchange factors (GEFs) catalyze the exchange, and thus activate the GTPase. GTPase activation protein (GAP) increases the intrinsic rate of hydrolysis of the γ -phosphate on the GTP molecule. The γ -phosphate is cleaved, and the GTPase becomes GDP-bound and deactivated. The GAP also has downstream effectors and can be members of other protein complexes. Another important regulatory protein is the guanine dissociation inhibitor (GDI),

which is thought to sequester GDP and membrane-bound RhoGTPases in the cytoplasm.

Rho1, a member of the RhoGTPase family, has been shown to be a major player in cell polarity and wall biogenesis. Studies of Rho1 in *S. cerevisiae* and *S. pombe* have identified 6 functions, some of which may overlap: (1) the Cdc42 cascade responsible for polarity establishment is linked to a Rho1-4 cascade for recruitment of actin and cytoskeletal components for bud emergence (Chant and Stowers, 1995); (2) Rho1-GTP binds to Bni1, an actin polymerizing protein, to regulate actin organization (Imamura et al., 1997); (3) exocytosis is mediated by the multiprotein exocyst complex which includes Sec3. Sec3 is a direct downstream effector of Rho1-GTP (Guo et al., 2001); (4) Rho1 and Cdc42 mediate the docking stage of vacuole fusion in endocytosis (Eitzen et al., 2001); (5) Rho1-GTP is part of the (1–3) β -D-glucan synthase complex that functions to generate cell wall (1–3) β -D-glucans (Arellano et al., 1996); and (6) stress activates Rho1 which lies upstream of the cell wall integrity pathway. This pathway includes Pkc1, the MAP kinase signaling cascade, and many downstream effectors including chitin synthases and Fks1/Fks2, the catalytic subunits of the (1–3) β -D-glucan synthase complex (Harrison et al., 2001).

In filamentous fungi, *RHO1* homologs have been cloned from *Aspergillus fumigatus* (*AfRHO1*) and *A. gossypii* (*Agrho1*). In *A. fumigatus*, *AfRHO1* and *AfFKS1* were shown to encode subunits of the (1–3) β -D-glucan synthase cell wall biosynthetic complex and to localize to hyphal apices (Beauvais et al., 2001). In cytological studies, the short-lived *A. gossypii Agrho1* deletion mutant exhibited irregularly shaped hyphae with varying intensities of calcofluor staining and an uneven distribution of nuclei, leading to the suggestion that *Agrho1* is involved in polar hyphal growth (Wendland and Philippsen, 2001).

To further investigate the role of Rho1 in filamentous fungi, the *A. nidulans* homologue *rhoA* was cloned and mutants were created and characterized. Results suggest that *rhoA* plays roles in polar growth, branching pattern and construction of the cell wall.

2. Materials and methods

2.1. Strains and growth medium

All strains used in this study are detailed in Table 1. Complete and minimal media with appropriate supplements were used (Kafer, 1977). For all microscopic examination, conidia were inoculated onto coverslips in liquid medium, incubated at the appropriate time and temperature, fixed, stained, and examined as previously described (Momany et al., 1999). For phenotypic, polar growth studies and branching studies,

Table 1
Aspergillus nidulans strains

Strain	Genotype
A773 ^a	<i>pyrG89; wA3; pyroA4</i>
AGG1	A773 + pGG2 (<i>rhoA</i> ^{G14V}) and pRG3AMA1 (co-transformation plasmid)
AGG2 ^b	A773 + pGG2 (<i>rhoA</i> ^{G14V}) and pRG3AMA1 (co-transformation plasmid)
AGG3 ^b	A773 + pGG5 (<i>rhoA</i> ^{E40I}) and pRG3AMA1 (co-transformation plasmid)
AGG5	A773 + pGG5 (<i>rhoA</i> ^{E40I}) and pRG3AMA1 (co-transformation plasmid)
AGG6	A773 + pGG5 (<i>rhoA</i> ^{E40I}) and pRG3AMA1 (co-transformation plasmid)
AGG7	A773 + pGG5 (<i>rhoA</i> ^{E40I}) and pRG3AMA1 (co-transformation plasmid)

^a Obtained from Fungal Genetics Stock Center, Department of Microbiology, University of Kansas Medical Center, Kansas City, Kansas 66160-7420.

^b Strains used in this study for phenotypic and cell wall analysis.

conidia were incubated at 42 °C for 5–7, 10, 14 or 20 h as noted.

2.2. Molecular techniques

Saccharomyces cerevisiae Rho1 amino acid sequence (Accession No. NC001148.1) was used to search the *A. nidulans* EST database (<http://www.genome.ou.edu/fungal.html>). A 450 bp sequence encoding a predicted protein with 89% similarity to the *S. cerevisiae* amino acid sequence was found. The *A. nidulans* EST sequence was used to search the NCBI database. The search confirmed that the sequence encoded a protein that was most similar to other Rho1 homologs. Primers 5′CAC TTCTGCCAGGGTCTC3′ and 5′CAAACCAAATCC ATCTCCC3′ were generated from the *A. nidulans* EST sequence and used to amplify a 400 bp fragment from *A. nidulans* wild type genomic DNA. The 400 bp fragment was radiolabelled and used as a probe to screen an *A. nidulans* chromosome specific cosmid library (Brody et al., 1991). Two positive clones L30A02 and W12C10 were isolated from the screen. Full-length genomic sequence including flanking regions was obtained from cosmid L30A02 through primer walking. Sequencing was performed using the Big Dye 2.0 kit (Perkin–Elmer Applied Biosystems, Boston, MA) and an ABI Prism 310 sequencer (Applied Biosystems, Foster City, CA). Analysis of sequences was performed using LaserGene software (DNASTAR, Madison, WI). Protein sequence was predicted based on homologous Rho1 proteins and the presence of consensus splice sites (Ballance, 1986). No cDNAs were isolated. *A. nidulans rhoA* sequences have been deposited with GenBank (Accession No. AAK08118).

2.3. Generation of *rhoA* mutants

A 2.3 kb fragment containing *rhoA* was PCR amplified from L30A02. The PCR product was cloned into the pGEM-T vector (Promega, Madison, Wisconsin) and named pGG1. Mutagenesis was performed using a site-directed mutagenesis kit (Stratagene, Cedar Creek,

TX) with mutagenic primers G14V (5′GCTTGTG ATCGTTGGTGTATGTTGCCTGCGGTAAGACCTG TC3′) and E40I (5′CTACGTCCCCACCGTCTT TATT AACTACGTTGCCGATGTTG3′). Base mismatches are underlined. Site directed mutagenesis was performed on pGG1 (*rhoA*) to generate pGG2 (*rhoA*^{G14V}) and pGG5 (*rhoA*^{E40I}). Constructs were verified by sequencing. To generate mutant *rhoA* strains, DNA from the insert region of pGG2 and pGG5 was gel purified and co-transformed with the marker plasmid pRG3-AMA1 containing the *pyr4* gene into *A. nidulans* strain A773 using standard protocols (Yelton et al., 1984). Approximately 500 *pyr*⁺ transformants from the pGG2 (*rhoA*^{G14V}) transformation were screened using a calcofluor plate assay as previously described (Harris et al., 1994). Approximately 1000 *pyr*⁺ transformants from the pGG5 (*rhoA*^{E40I}) transformation were replica plated onto minimal medium and incubated at 30 and 42 °C. The plates were then visually screened by stereoscope. Putative mutant strains were named AGG1 and AGG2 for *rhoA*^{G14V} and AGG3, AGG4, AGG5, AGG6, and AGG7 for *rhoA*^{E40I}. Genomic DNA was isolated from chosen transformants and wild type and digested with *SacI*. Southern blot hybridization was performed with a 400 bp *rhoA* fragment as probe.

Ectopic integrations of two *rhoA*^{G14V} and four *rhoA*^{E40I} strains were confirmed by allele specific restriction enzyme digestion of PCR amplified regions. Sequence analysis of wild type and *rhoA*^{G14V} showed the destruction of a *BanI* restriction site (5′G ↓ GTGCC3′) in the *rhoA*^{G14V} mutant. The region containing this restriction site was amplified by PCR from pGG1 (*rhoA*), pGG2 (*rhoA*^{G14V}), A773 genomic DNA, AGG1, and AGG2 genomic DNA. Primers 5′CGGTGTAGA AACTGGGCG3′ and 5′CTTCTTGCGGACTTCC TC3′ were used to amplify both *rhoA* and *rhoA*^{G14V} alleles. The PCR fragments were digested with *BanI* and analyzed on a 2.5% agarose gel. Sequence analysis of wild type and *rhoA*^{E40I} showed the creation of a *Tru9I* restriction site (5′TAT ↓ T3′) in the *rhoA*^{E40I} mutant. The region containing this restriction site was amplified by PCR from pGG1 (*rhoA*), pGG5 (*rhoA*^{E40I}), A773,

AGG3, AGG5, AGG6, and AGG7. Primers 5'CCCGTGCAGCGTCTTCTC3' and 5'CTTCTTGCGGACTTCCTC3' were used to amplify both *rhoA* and *rhoA*^{E40I} alleles. The PCR fragments were digested with *Tru9I* and analyzed on a 1.0% agarose gel.

2.4. Cell wall analysis

Cell wall from A773, AGG2 (*rhoA*^{G14V}), and AGG3 (*rhoA*^{E40V}) was isolated from an overnight culture as previously described (Guest and Momany, 2000). Wall samples were prepared, trimethylsilylated (TMS), resolved and analyzed using gas chromatography and mass spectroscopy at the Complex Carbohydrate Research Center at the University of Georgia as previously described (Guest and Momany, 2000).

Sensitivity to cell wall disrupting agents was determined by incubating conidia in 1 ml complete medium plus 0–400 μ M calcofluor (Bayer, Research Triangle Park, NC) or 0–100 μ M caspofungin acetate (CANCIDAS, Merck, Whitehouse Station, NJ). All incubations were at 42 °C.

Samples were prepared for transmission electron microscopy and gold labeled as previously described (Momany et al., 2002). Briefly, A773 and AGG2 (*rhoA*^{G14V}) spores were inoculated on dialysis membrane placed on complete medium for 14 h at 42 °C. The dialysis membrane with adhering hyphae were fixed by freeze substitution, flat embedded in Embed/Araldite resin (Electron Microscopy Sciences, Ft. Washington, Pennsylvania) and sectioned using an RMC 6000XL ultramicrotome. Grids were examined in a Zeiss EM 902A TEM. Wheat germ agglutinin gold label (Sigma, Lectin from *Triticum vulgare*), which binds specifically to *N*-acetylglucosamine, was used to visualize chitin.

3. Results

3.1. *rhoA* encodes a highly conserved *RHO1* homolog

A search of the *A. nidulans* EST database revealed a 400 bp sequence predicted to encode a protein with 89% similarity to the *S. cerevisiae* Rho1 (<http://www.genome.ou.edu/fungal.html>). This conserved region was PCR amplified from *A. nidulans* genomic DNA, radio-labeled and used to probe *A. nidulans* genomic chromosome specific cosmid libraries (Prade et al., 1997). Two Chromosome V clones hybridized with the probe and the relevant region was sequenced from one. The *A. nidulans* *RHO1* homolog was named *rhoA*. *rhoA* spans an open reading frame of 870 bp and, based on homology with other *RHO1* genes and the *A. nidulans* intron splicing sequence (Ballance, 1986), is predicted to contain 5 exons and 4 introns. RhoA is 89% similar to *S. cerevisiae* Rho1 and is predicted to encode a 196 amino-acid protein (Fig. 1) with domains previously shown to be necessary in *S. cerevisiae* Rho1 function (Saka et al., 2001). These domains include the conserved GDGACGKT region (Fig. 1) responsible for the proper positioning and transition of the GTP/GDP molecule, and the YVPTVFENY effector region, responsible for binding of the regulatory GTPase activating protein (GAP) and other effectors (Hall, 2000).

3.2. *rhoA* mutants have ectopically integrated mutant alleles

Rho1 is a single copy, essential protein, and attempted deletions have been unsuccessful in all haploid fungal systems tested, including *A. fumigatus* and *A. gossypii* (Beauvais et al., 2001; Wendland and Phil-

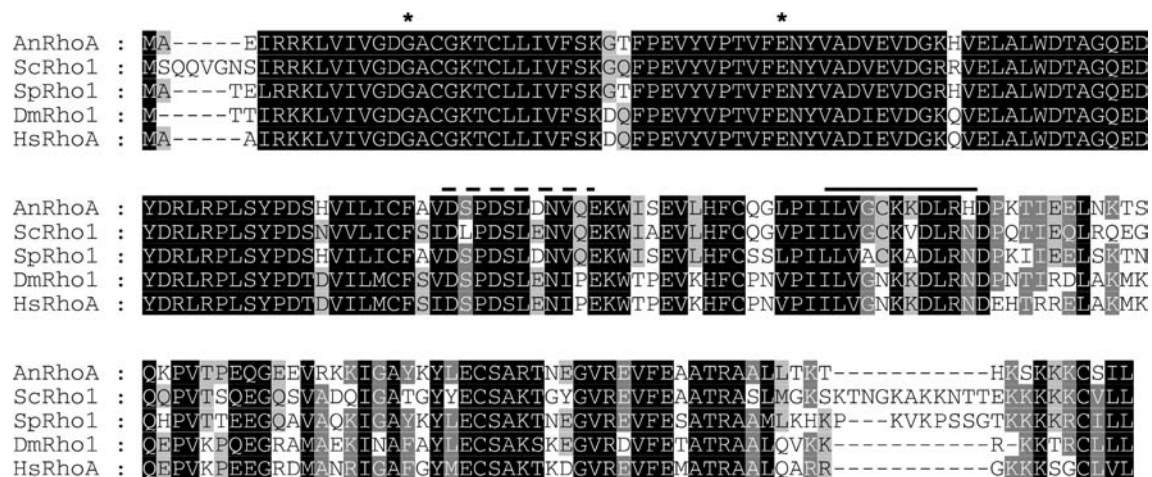


Fig. 1. Protein sequence alignment of Rho1 homologs. Predicted protein sequences from *A. nidulans* (An; AAK08118), *S. cerevisiae* (Sc; NP015491), *S. pombe* (Sp; T37769), *Drosophila melanogaster* (Dm; NP599136), and *Homo sapiens* (Hs; NP001655) are shown. Asterisks indicate amino acids mutated in this study, G14V and E40I. Black shading denotes five similar residues, dark gray denotes four similar, and light gray denotes three similar.

ippsen, 2001). A deletion of *rhoA* was therefore not attempted in this study. Instead, to examine the role of *rhoA* in growth and development, dominant constitutively active *rhoA*^{G14V} and dominant *rhoA*^{E40I} alleles were generated on plasmids by site-directed mutagenesis. The equivalent alleles were previously determined to affect polar growth and cell wall integrity in the yeasts *S. cerevisiae*, *S. pombe*, and *Cryptococcus neoformans* (Arellano et al., 1996; Chang and Penoyer, 2000; Kohno et al., 1996). Wild type *A. nidulans* strain A773 (*pyrG*⁻) was co-transformed with pRG3AMA1 (*pyr4*⁺) and mutant *rhoA* from either pGG2 (*rhoA*^{G14V}) or pGG5 (*rhoA*^{E40I}). *Pyr*⁺ transformants were incubated on plates with calcofluor (*rhoA*^{G14V} experiments) or without calcofluor (in *rhoA*^{E40I} experiments) and visually screened using a stereoscope. Calcofluor White is a dye that specifically binds to chitin and causes it to fluoresce under UV light (Cid et al., 1995). Twelve potential *rhoA*^{G14V} strains were initially chosen based on calcofluor brightness and a range of abnormal hyphal morphologies. Ten potential *rhoA*^{E40I} strains were chosen based on a range of abnormal colony morphologies. All putative mutant strains were streaked multiple times to determine stability of the mutant phenotype and analyzed by Southern blot. Two *rhoA*^{G14V} strains (AGG1 and AGG2) and 4 *rhoA*^{E40I} strains (AGG3, AGG5, AGG6, and AGG7) contained the native *rhoA* and 1–4 copies of the mutant allele. No homologous integrants were found (data not shown).

Ectopic integration of *rhoA* mutant strains was confirmed by allele specific restriction enzyme digestion of PCR amplified regions (Fig. 2). A *BanI* site is present in the *rhoA* allele but destroyed in the *rhoA*^{G14V} allele. A 740 bp fragment was amplified by PCR from both wild type and *rhoA*^{G14V} strains (AGG1 and AGG2) and cut with *BanI*. Resolution of both band sizes of 700 bp (wild type) and 740 bp (*rhoA*^{G14V}) indicated the presence of wild type and mutant alleles in both AGG1 and AGG2 (Fig. 2A). Preliminary microscopic characterization of AGG1 and AGG2 indicated that both strains were virtually identical, thus only AGG2 was used to further characterize the *rhoA*^{G14V} allele.

A *Tru9I* site is absent from the wild type *rhoA* allele and generated in the *rhoA*^{E40I} allele. A 610 bp fragment was amplified by PCR from both wild type and *rhoA*^{E40I} strains (AGG3, AGG5, AGG6, and AGG7) and cut with *Tru9I*. Resolution of bands of 610 bp (wild type) and 450 bp (*rhoA*^{E40I}) indicated presence of wild type and mutant alleles in AGG3, AGG5, AGG6, and AGG7 (Fig. 2B). Preliminary microscopic characterizations of AGG3, AGG5, AGG6, and AGG7 indicated that these strains were virtually identical, thus only AGG3 was used to further characterize the *rhoA*^{E40I} allele.

3.3. *rhoA* mutants are delayed or accelerated in germ tube emergence

Growth at early time points was examined to determine what percentage of the *rhoA* mutant population developed primary, secondary, and tertiary germ tubes and lateral branches relative to wild type. In wild type, a conidium breaks dormancy and after 4 h of incubation a primary germ tube emerges. After 6–8 h of incubation a secondary germ tube appears, usually in a bipolar pattern (Harris et al., 1999; Momany and Taylor, 2000). By 9 h a lateral branch might emerge from the primary germ tube and by 10 h, a tertiary germ tube might emerge from the original conidium (B. Shaw and M. Momany, unpublished results).

The *rhoA*^{G14V} strain AGG2 germinated slowly, was calcofluor bright, and grew slowly relative to wild type (Figs. 3B and E). After 6 h incubation, approximately 90% of wild type cells showed polar growth compared with approximately 20% of *rhoA*^{G14V} cells (Fig. 4). By 20 h of incubation, approximately 95% of the *rhoA*^{G14V} population developed a short germ tube (data not shown). By 48 h colonies appeared to be the same size as wild type (Fig. 3H).

The *rhoA*^{E40I} strain AGG3 was accelerated in the emergence of secondary and tertiary germ tubes, and lateral branches. By 6 h of incubation, approximately 4% of wild type cells and 35% of *rhoA*^{E40I} cells had a secondary germ tube (Figs. 3A, C and 5). By 7 h,

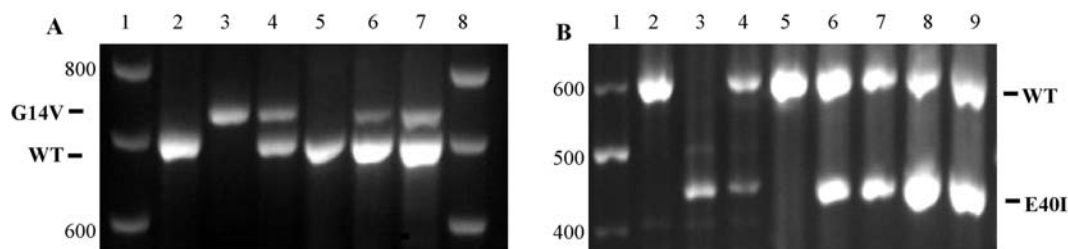


Fig. 2. *rhoA* mutants are the result of ectopic integrations. DNA was amplified from wild type or *rhoA* mutants, incubated with restriction enzyme indicated and electrophoresed. (A) Lanes 1 and 8, 100 bp ladder. Lanes 2–7, cut with *BanI*. Lane 2, product amplified from pGG1; lane 3, pGG2 (*rhoA*^{G14V}); lane 4, mixture pGG1 and pGG2; lane 5, A773 genomic DNA; lanes 6, AGG1; and lane 7, AGG2. (B) Lane 1, 100 bp ladder. Lanes 2–9, cut with *Tru9I*. Lane 2, product amplified from pGG1; lane 3, pGG5 (*rhoA*^{E40I}); lane 4, mixture of lanes 2 and 3; lane 5, A773; and lanes 6–9, product amplified from AGG3, AGG5, AGG6, and AGG7 genomic DNA, respectively.

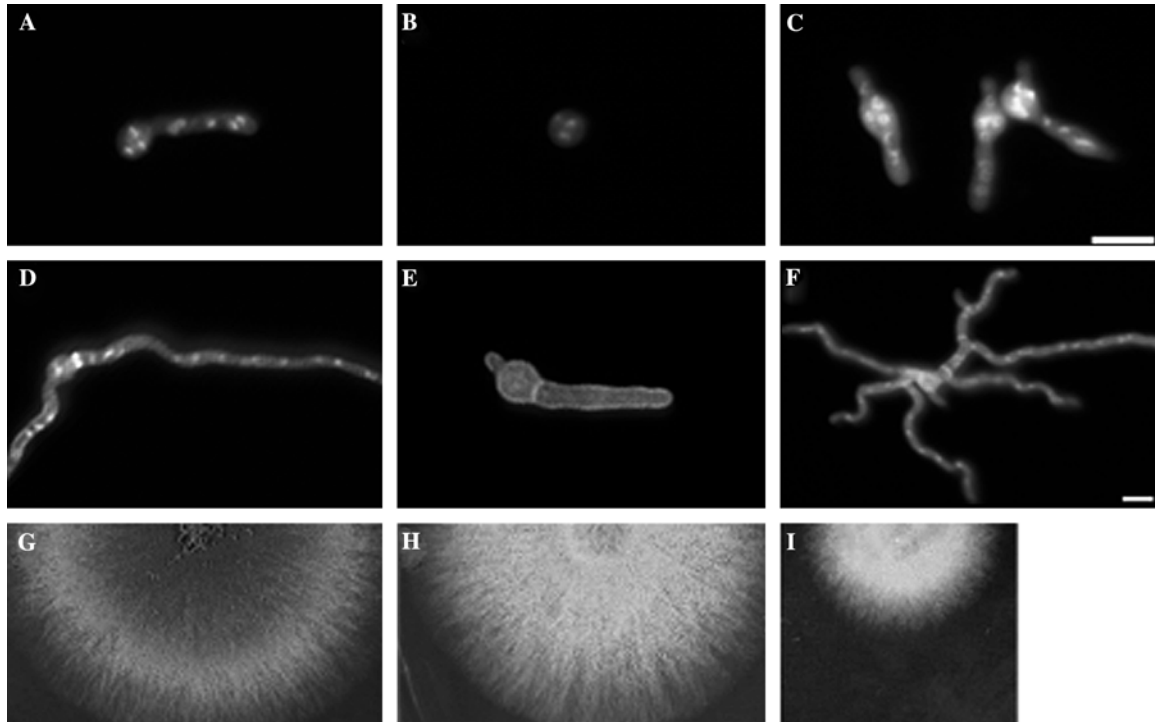


Fig. 3. *rhoA* mutants have abnormal morphology. *rhoA* mutants were inoculated onto coverslips or solid complete medium and incubated at 42 °C for 6 h (A–C), 10 h (D–F) or 48 h (G–I). Strains were fixed and stained with Calcofluor and Hoechst 33258 to visualize chitin and nuclei (A–F) or photographed on solid medium (G–I). (A, D, G) wild type; (B, E, H) AGG2 (*rhoA*^{G14V}); (C, F, I) AGG3 (*rhoA*^{E40I}). Bar, 10 μ M.

approximately 10% of the wild type and 65% of the *rhoA*^{E40I} population had a secondary germ tube. By 7 h 25% of *rhoA*^{E40I} cells and no wild type cells had a tertiary germ tube or lateral branch. By 10 h, most *rhoA*^{E40I} cells were clearly hyperbranching (Fig. 3F). By 48 h colonies appeared compact relative to wild type (Fig. 3I).

3.4. *rhoA* mutants have an abnormal branching pattern

A general morphological characteristic of wild type *A. nidulans* is the compartmentalization of hyphae by

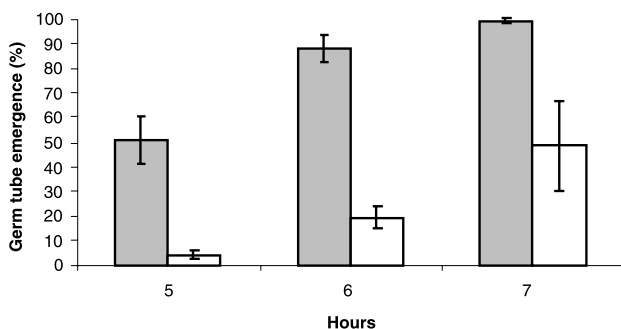


Fig. 4. *rhoA*^{G14V} mutant is delayed in germ tube emergence. Spores from wild type (gray) and *rhoA*^{G14V} (white) were inoculated onto coverslips in complete medium and incubated at 42 °C for 5, 6, and 7 h. For each time point, 100 spores were counted. The count was repeated three times.

septa and the emergence of lateral branches in a basal to apical progression. Typically one lateral branch per compartment is observed (Fig. 6A). *rhoA*^{G14V} was delayed in branching, but after an incubation of approximately 20 h, branches were observed emerging from the initial germ tube in a clustered manner (Fig. 6B). *rhoA*^{E40I} hyphae were clearly compartmentalized, but did not have a regular branching pattern (Fig. 6C).

3.5. *rhoA* mutants have an altered cell wall

In *S. cerevisiae*, cell wall is laid down during normal polar growth and in response to stress, which triggers the cell wall integrity pathway. Both processes involve the function of Rho1 (Jung and Levin, 1999; Pruyne and Bretscher, 2000). In other fungi mutant alleles equivalent to *rhoA*^{G14V} and *rhoA*^{E40I} have cell wall defects (Arellano et al., 1999; Chang and Penoyer, 2000; Drgonova et al., 1999). Mutants with altered cell walls can often be restored to a wild type phenotype by the addition of osmoticum to the medium. However, incubation with sorbitol, sucrose, NaCl, and KCl did not change the colony phenotypes of *rhoA*^{E40I} or *rhoA*^{G14V} mutants (data not shown). However, the observation that *rhoA*^{G14V} was very calcofluor bright and *rhoA*^{E40I} showed tip lysis when incubated for greater than 14 h suggested that *rhoA* mutant alleles might have abnormal cell walls. Cell walls of wild type, *rhoA*^{G14V} and *rhoA*^{E40I}

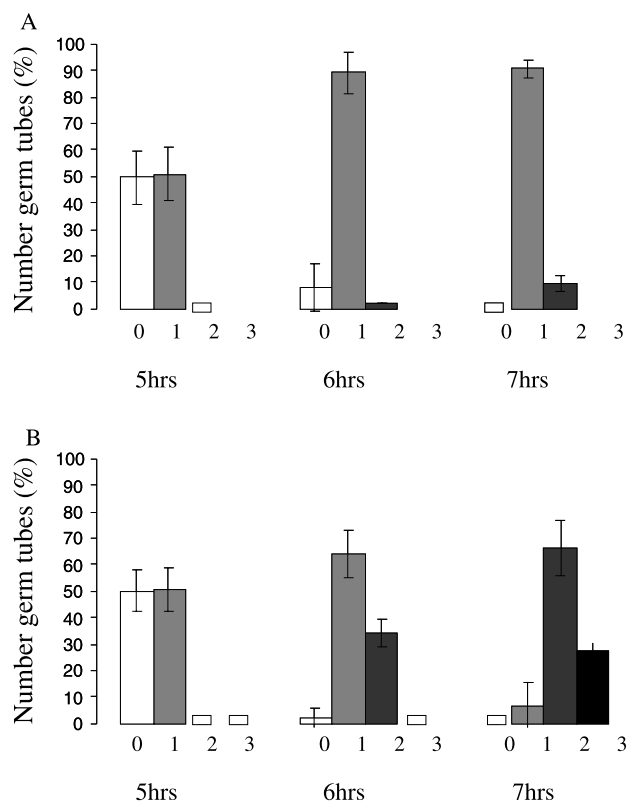


Fig. 5. *rhoA^{E40I}* mutant branching is accelerated. Spores from wild type (A) and *rhoA^{E40I}* (B) were inoculated onto coverslips in complete medium and incubated at 42 °C for 5, 6, and 7 h. For each time point, 100 spores were counted. 0 germ tubes, white bar; one germ tube, 1, light gray bar; a primary and a secondary germ tube, 2, dark gray bar; and a primary, secondary, tertiary or lateral branch, 3, black bar. The count was repeated three times.

strains were isolated and analyzed by gas chromatography/mass spectroscopy (Table 2). Wild type cell wall composition was consistent with previous studies (Guest and Momany, 2000) except for the small amount of rhamnose detected. Relative to wild type, *rhoA^{G14V}* showed a 46% reduction in galactose, a 49% reduction in mannose, and a 53% increase in *N*-acetylglucosamine, the monomer of chitin. *rhoA^{E40I}* showed a 36% reduction in galactose, a 55% reduction in mannose, and a 37% increase in *N*-acetylglucosamine relative to wild type.

Table 2
Carbohydrate in wild type and mutant cell walls^a

Strain	Glucose	Galactose	Mannose	Rhamnose	GlcNac ^b
A28	71.3	9.1	8.6	1.9	9.1
<i>Anrho1^{G14V}</i>	64.0	4.9	4.4	n.d. ^c	19.0
<i>Anrho1^{E40I}</i>	69.6	5.9	3.9	n.d. ^c	14.3

^a Average percent of individual sugar present in total carbohydrate based on GC/MS chromatographic area. Analysis was repeated two times with essentially identical results.

^b *N*-Acetylglucosamine.

^c None detected.

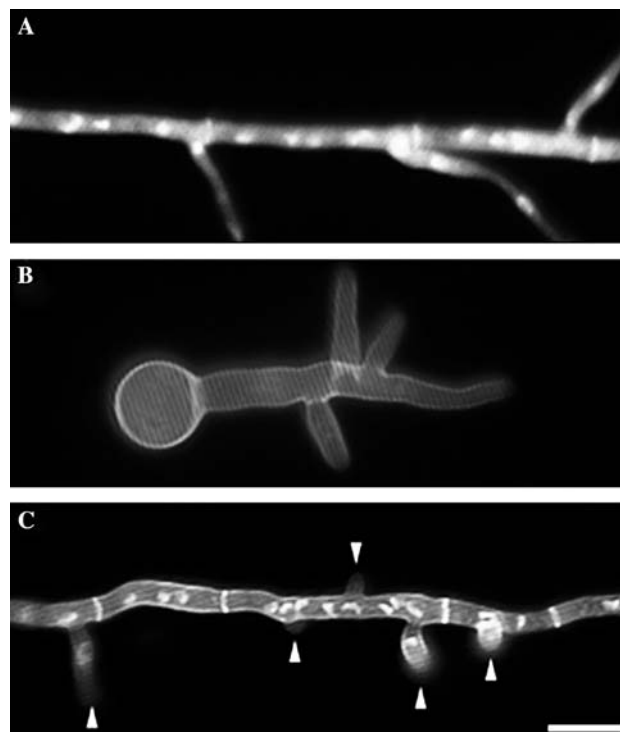


Fig. 6. *rhoA* mutants have an abnormal branch emergence pattern. Strains were inoculated onto coverslips in complete medium, incubated at 42 °C, fixed and stained with Calcofluor and Hoescht 33258 to visualize chitin and nuclei. (A) Wild type incubated for 20 h; (B) *Anrho1^{G14V}* mutant incubated for 20 h; (C) *Anrho1^{E40I}* mutant incubated for 12 h, arrows indicate emerging branches. Bar, 10 μM.

Wild type and mutant strains were incubated with the cell wall altering agents calcofluor, which binds chitin, and caspofungin acetate, which inhibits (1–3)β-D-glucan synthase. *rhoA^{E40I}* cells were hypersensitive to calcofluor and caspofungin acetate, while *rhoA^{G14V}* cells showed wild type sensitivity to these agents. To determine whether calcofluor brightness in the *rhoA^{G14V}* mutant was due to a thick wall, hyphae were examined by transmission electron microscopy (Fig. 7). Wild type cell walls were approximately 12 nm wide (white asterisk) and *rhoA^{G14V}* cell walls were approximately 40 nm wide (black asterisk). The cell walls of the mutant also showed a less dense staining pattern, possibly reflecting a difference in cell wall architecture. Labeling of sections

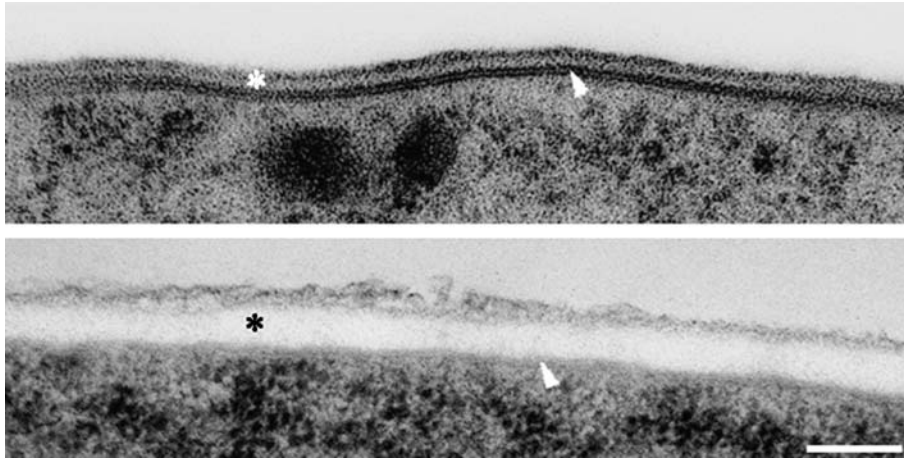


Fig. 7. Transmission electron micrograph of near median sections through a wild type (top) and *Anrho1*^{G14V} mutant (bottom) hypha. Arrows denote the plasma membrane and asterisks indicate cell wall. Bar, 65 nm.

with wheat germ agglutinin (WGA) gold conjugate—a lectin that specifically binds chitin—confirmed the thick *rhoA*^{G14V} wall contained chitin (data not shown).

4. Discussion

4.1. *rhoA* plays a role in emergence of the primary germ tube

At early time points AGG2, the strain carrying *rhoA*^{G14V}, showed a marked delay in primary germ tube emergence while AGG3, the strain carrying *rhoA*^{E40I}, showed no change in primary germ tube emergence relative to wild type. These contrasting phenotypes likely resulted because the mutations lie in different functional domains of RhoA. The *rhoA*^{G14V} mutation renders the protein constitutively active by preventing the hydrolysis of GTP. The observed delay in germ tube emergence could be explained by either a delay in marking the spot coupled with normal germ tube emergence or by normal marking of the spot coupled with delayed germ tube emergence. In either case, the *rhoA*^{G14V} mutation might exert its effect via a cell wall integrity pathway similar to that of *S. cerevisiae* (Jung and Levin, 1999). In *S. cerevisiae*, stress causes actin to depolarize so that the cell can adjust to external conditions before resuming polar growth (Delley and Hall, 1999). This actin depolarization changes the distribution of numerous cell wall components, most notably Fks1p—a member of the β -glucan synthase complex. After the cell has adjusted to the external environment, actin repolarizes and normal growth continues. The constitutively active *rhoA*^{G14V} may inappropriately signal cell stress and thus delay repolarization.

The *rhoA*^{E40I} mutation perturbs the GAP binding domain and likely disturbs downstream targets of the

GAP protein, targets that have not yet been identified in *A. nidulans*. The normal emergence of the primary germ tube in *rhoA*^{E40I} mutants suggests that GAP targets are not important for primary germ tube emergence.

4.2. *rhoA* plays a role in emergence of secondary germ tubes and branches

Both *rhoA* mutants branched, but not in the normal pattern. Emergence of lateral branches in the *rhoA*^{G14V} strain was delayed and branches were clustered while emergence of secondary and tertiary germ tubes and branches in the *rhoA*^{E40I} strain was accelerated and lateral branches emerged in irregular numbers. Two proteins have recently been identified in *A. nidulans* as possible markers for branch emergence, the formin SepA, which is responsible for proper actin assembly and organization (Sharpless and Harris, 2002) and the septin AspB, which is a member of a family of scaffold proteins that organize areas of new growth (Westfall and Momany, 2002). AspB localizes to sites of emerging secondary germ tubes and lateral branches, but not to emerging primary germ tubes (Westfall and Momany, 2002). This pattern of AspB localization suggests that emergence of secondary germ tubes and branches differs from the emergence of the primary germ tube. The fact that *rhoA*^{E40I} mutants show altered emergence of secondary germ tubes and branches, but are normal with regard to the primary germ tube supports this idea.

Localization of both SepA and AspB is actin dependent. Rho1 has been shown to interact with Bni1, the *S. cerevisiae* homolog of SepA (Imamura et al., 1997). A yeast two-hybrid study placed *S. cerevisiae* septins Cdc11 and Cdc12 as indirect downstream effectors of Rho1 (Drees et al., 2001). By analogy, it seems likely that *A. nidulans* RhoA also lies upstream of SepA and AspB and that these two proteins are dependent on proper functioning of RhoA.

4.3. *rhoA* plays a role in cell wall deposition

Both *rhoA* mutations likely affect the cell wall integrity pathway. In *S. cerevisiae* cell wall is laid down during normal vegetative growth and in response to stress activation of the cell wall integrity pathway (Davenport et al., 1995; Lipke and Ovalle, 1998). Genetically, *S. cerevisiae* Rho1 lies between the cell wall stress sensors Mid2p and Wsc1p and the kinase Pkc1p. Working through a MAPK cascade, Pkc1p triggers the cell wall integrity pathway (Jung and Levin, 1999). Downstream effectors induce the enzymes responsible for the production of (1–3) β -D-glucans, chitin, and other wall components. The increased *N*-acetylglucosamine in both mutants is consistent with a stress-triggered increase in chitin. Indeed, overexpression of the *S. cerevisiae* MAPK pathway member MKK1 led to a 30-fold increase in expression of genes involved in chitin and glucan synthesis (Jung and Levin, 1999). Chitin levels increased from 2% to 20%, and the incorporation of cell wall proteins was altered in *S. cerevisiae* in response to stress (Smits et al., 1999).

The difference in wall-related phenotypes of the mutants is probably the result of the disruption of different functional domains of RhoA. The constitutively active *rhoA*^{G14V} mutant was calcofluor bright, had thick walls and was resistant to cell wall disrupting agents, as one would expect if the stress response were constitutive. The GAP binding region *rhoA*^{E40I} mutant lysed easily as did analogous mutants in *S. cerevisiae* and *C. neoformans* (Chang and Penoyer, 2000; Saka et al., 2001). The *rhoA*^{E40I} mutant was also sensitive to cell wall disrupting agents suggesting that downstream targets of GAP might be important in wall synthesis or deposition.

Acknowledgments

This work was supported by DOE Biosciences Grant DE-FG02-97ER20275 to M.M. We thank Merck for supplying Caspofungin Acetate and Brian Shaw for helpful discussions on the project.

References

- Arellano, M., Coll, P.M., Perez, P., 1999. RHO GTPases in the control of cell morphology, cell polarity, and actin localization in fission yeast. *Microsc. Res. Tech.* 47, 51–60.
- Arellano, M., Duran, A., Perez, P., 1996. Rho1 GTPase activates the (1–3) β -D-glucan synthase and is involved in *Schizocaccharomyces pombe* morphogenesis. *EMBO J.* 15, 4584–4591.
- Ballance, D.J., 1986. Sequences important for gene expression in filamentous fungi. *Yeast* 2, 229–236.
- Beauvais, A., Bruneau, J.M., Mol, P.C., Buitrago, M.J., Legrand, R., Latge, J.P., 2001. Glucan synthase complex of *Aspergillus fumigatus*. *J. Bacteriol.* 183, 2273–2279.
- Boyce, K.J., Hynes, M.J., Andrianopoulos, A., 2001. The *CDC42* homolog of the dimorphic fungus *Penicillium marneffeii* is required for correct cell polarization during growth but not development. *J. Bacteriol.* 183, 3447–3457.
- Brody, H., Griffith, J., Cuticchia, A.J., Arnold, J., Timberlake, W.E., 1991. Chromosome-specific recombinant DNA libraries from the fungus *Aspergillus nidulans*. *Nucleic Acids Res.* 19, 3109.
- Chang, Y.C., Penoyer, L.A., 2000. Properties of various *RHO1* mutant alleles of *Cryptococcus neoformans*. *J. Bacteriol.* 182, 4987–4991.
- Chant, J., Stowers, L., 1995. GTPase cascades choreographing cellular behavior: movement, morphogenesis, and more. *Cell* 81, 1–4.
- Cid, V.J., Duran, A., del Rey, F., Snyder, M.P., Nombela, C., Sanchez, M., 1995. Molecular basis of cell integrity and morphogenesis in *Saccharomyces cerevisiae*. *Microbiol. Rev.* 59, 345–386.
- Davenport, K.R., Sohaskey, M., Kamada, Y., Levin, D.E., Gustin, M.C., 1995. A second osmosensing signal transduction pathway in yeast. *J. Biol. Chem.* 270, 30157–30161.
- Delley, P.-A., Hall, M.N., 1999. Cell wall stress depolarizes cell growth via hyperactivation of RHO1. *J. Cell Biol.* 147, 163–174.
- Drees, B.L., Sundin, B., Brazeau, E., et al., 2001. A protein interaction map for cell polarity development. *J. Cell Biol.* 154, 549–571.
- Drgonova, J., Drgon, T., Roh, D.-H., Cabib, E., 1999. The GTP-binding protein RhoA is required for cell cycle progression and polarization of the yeast cell. *J. Cell Biol.* 146, 373–387.
- Eitzen, G., Thorngren, N., Wickner, W., 2001. RhoA and Cdc42p act after Ypt7p to regulate vacuole docking. *EMBO J.* 20, 5650–5656.
- Guest, G.M., Momany, M., 2000. Analysis of cell wall sugars in the pathogen *Aspergillus fumigatus* and the saprophyte *Aspergillus nidulans*. *Mycologia* 92, 1047–1050.
- Guo, W., Tamanoi, F., Novick, P., 2001. Spatial regulation of the exocyst complex by Rho1 GTPase. *Nat. Cell Biol.* 3, 353–360.
- Hall, A., 2000. GTPases. Oxford University Press, New York.
- Harris, S.D., 1997. The duplication cycle in *Aspergillus nidulans*. *Fung. Genet. Biol.* 22, 1–12.
- Harris, S.D., Hofmann, A.F., Tedford, H.W., Lee, M.P., 1999. Identification and Characterization of genes required for hyphal morphogenesis in the filamentous fungus *Aspergillus nidulans*. *Genetics* 151, 1015–1025.
- Harris, S.D., Morrell, J.L., Hamer, J.E., 1994. Identification and characterization of *Aspergillus nidulans* mutants defective in cytokinesis. *Genetics* 136, 517–532.
- Harrison, J.C., Bardes, E.S.G., Ohya, Y., Lew, D., 2001. A role for the Pkc1p/Mapk1p kinase cascade in the morphogenesis checkpoint. *Nat. Cell Biol.* 3, 417–420.
- Imamura, H., Tanaka, K., Hihara, T., Umikawa, M., Kamei, T., Takahashi, K., Sasaki, T., Takai, Y., 1997. Bni1p and Bnr1p: downstream targets of the Rho family small G-proteins which interact with profilin and regulate actin cytoskeleton in *Saccharomyces cerevisiae*. *EMBO J.* 16, 2745–2755.
- Jung, U.S., Levin, D.E., 1999. Genome-wide analysis of gene expression regulated by the yeast cell wall integrity signalling pathway. *Mol. Microbiol.* 34, 1049–1057.
- Kafer, E., 1977. Meiotic and mitotic recombination in *Aspergillus* and its chromosomal aberrations. *Adv. Genet.* 19, 33–131.
- Kohno, H., Tanaka, K., Mino, A., Umikawa, M., Imamura, H., Fujiwara, T., Fujita, Y., Hotta, K., Qadota, H., Watanabe, T., Ohya, Y., Takai, Y., 1996. Bni1p implicated in cytoskeletal control is a putative target of RhoA small GTP binding protein in *Saccharomyces cerevisiae*. *EMBO J.* 15, 6060–6068.
- Lew, D., Reed, S.I., 1995. Cell cycle control of morphogenesis in budding yeast. *Cur. Opin. Genet. Dev.* 5, 17–23.
- Lipke, P.N., Ovalle, R., 1998. Cell wall architecture in yeast: new structure and new challenges. *J. Bacteriol.* 180, 3735–3740.
- Momany, M., 2002. Polarity in filamentous fungi: establishment, maintenance and new axes. *Curr. Opin. Microbiol.* 5, 580–585.

- Momany, M., Richardson, E.A., Van Sickle, C., 2002. Mapping woronin body position in *Aspergillus nidulans*. *Mycologia* 94, 260–266.
- Momany, M., Taylor, I., 2000. Landmarks in the early duplication cycles of *Aspergillus fumigatus* and *Aspergillus nidulans*: polarity, germ tube emergence and septation. *Microbiology* 146, 3279–3284.
- Momany, M., Westfall, P.J., Abramowsky, G., 1999. *Aspergillus nidulans* *swo* mutants show defects in polarity establishment, polarity maintenance and hyphal morphogenesis. *Genetics* 151, 557–567.
- Osherov, N., May, G.S., 2001. The molecular mechanisms of conidial germination. *FEMS Microbiol. Lett.* 199, 153–160.
- Prade, R.A., Griffith, J., Kochut, K., Arnold, J., Timberlake, W.E., 1997. In vitro reconstruction of the *Aspergillus nidulans* genome. *Proc. Natl. Acad. Sci. USA* 94, 14564–14569.
- Pruyne, D., Bretscher, A., 2000. Polarization of cell growth in yeast I. Establishment and maintenance of polarity states. *J. Cell Sci.* 113, 365–375.
- Riquelme, M., Roberson, R.W., McDaniel, D.P., Bartnicki-Garcia, S., 2002. The effects of *ropy-1* mutation on cytoplasmic organization and intracellular motility in mature hyphae of *Neurospora crassa*. *Fung. Genet. Biol.* 37, 171–179.
- Saka, A., Abe, M., Okano, H., Minemura, M., et al., 2001. Complementing yeast *rho1* mutation groups with distinct functional defects. *J. Biol. Chem.* 276, 46165–46171.
- Sharpless, K.E., Harris, S.D., 2002. Functional characterization and localization of the *Aspergillus nidulans* formin SEPA. *Mol. Biol. Cell* 13, 469–479.
- Smits, G.J., Kapteyn, J.C., van den Ende, H., Klis, F.M., 1999. Cell wall dynamics in yeast. *Curr. Opin. Microbiol.* 2, 348–352.
- Wendland, J., Philippsen, P., 2001. Cell polarity and hyphal morphogenesis are controlled by multiple Rho-protein modules in the filamentous ascomycete *Ashbya gossypii*. *Genetics* 157, 601–610.
- Westfall, P.J., Momany, M., 2002. *Aspergillus nidulans* septin AspB plays pre- and postmitotic roles in septum, branch, and conidiophore development. *Mol. Biol. Cell* 13, 110–118.
- Yelton, M.M., Hamer, J.E., Timberlake, W.E., 1984. Transformation of *Aspergillus nidulans* by using a *trpC* plasmid. *Proc. Natl. Acad. Sci. USA* 81, 1470–1474.